Chapter 13

Designing Image Analysis Pipelines in Light Microscopy: A Rational Approach

Ignacio Arganda-Carreras and Philippe Andrey

Abstract

With the progress of microscopy techniques and the rapidly growing amounts of acquired imaging data, there is an increased need for automated image processing and analysis solutions in biological studies. Each new application requires the design of a specific image analysis pipeline, by assembling a series of image processing operations. Many commercial or free bioimage analysis software are now available and several textbooks and reviews have presented the mathematical and computational fundamentals of image processing and analysis. Tens, if not hundreds, of algorithms and methods have been developed and integrated into image analysis software, resulting in a combinatorial explosion of possible image processing sequences. This paper presents a general guideline methodology to rationally address the design of image processing and analysis pipelines. The originality of the proposed approach is to follow an iterative, backwards procedure from the target objectives of analysis. The proposed goal-oriented strategy should help biologists to better apprehend image analysis in the context of their research and should allow them to efficiently interact with image processing specialists.

Key words Light microscopy, Image analysis, Image processing, Image segmentation, Watershed transform

1 Introduction

Continuous improvements and innovations in light microscopy techniques result in increasing amounts of image data. In parallel, formal approaches imported from mathematics, statistics, and computer science are progressively penetrating biological sciences. In light microscopy, quantitative image analysis can be used to answer many different questions about biological specimens. Automatizing image analysis by means of a set of consecutive techniques or *pipeline* presents three main advantages: first, it prevents the bias inherent to human vision; second, it grants the extraction of information that is not accessible by eye; and finally, it allows to process very large amounts of image data, otherwise unmanageable. Consequently, there is an increasing need for biologists to

Yolanda Markaki and Hartmann Harz (eds.), *Light Microscopy: Methods and Protocols*, Methods in Molecular Biology, vol. 1563, DOI 10.1007/978-1-4939-6810-7_13,

gain fundamental knowledge and practical experience to fully exploit acquired images and extract from these data as much quantitative and relevant information as possible.

However, there are two potential difficulties for biologists to use image analysis. The first one is that, as opposed to wet experiment protocols, there is no such thing as a standard image processing and analysis pipeline. An imaging experiment generally corresponds to a unique combination of biological system, sample preparation, microscopic apparatus, acquisition conditions, etc. It therefore requires the design of a specific image processing and analysis chain. Users are here confronted to the combinatorial explosion that results from the numerous methods available at each step in a typical image processing pipeline. The second difficulty is that image processing textbooks and introductory articles are generally structured according to the mathematical or computational underlying principles and following the chronological order of application of operations. This is not the most appropriate approach for biologists, who focus on end analysis objectives and output measures rather than on the technical means, and their theoretical foundations, to attain these goals.

We present here a general approach to help biologists design specific pipelines suited to their scientific problems. The originality of this methodology is to put the emphasis on the ultimate goals of the analysis and to incrementally introduce the intermediate processing steps according to a binary decision scheme. This shift of focus from the "how" to the "why" of image analysis leads to completely reverse the traditional order of considering image processing steps at the design stage. Though this may sound paradoxical in the first place, several years of teaching and research experience demonstrate that the proposed iterative, goal-oriented approach is both natural and efficient.

2 Materials

2.1 Hardware Equipment

The methods described here can be run on any modern computer with standard configuration. However, applying these methods to large volume images (roughly, from 1 Gb and more) may require above standard RAM equipment. A high performance accelerated graphics card may also be required, especially if demanding 3D rendering is desired. Images can be stored locally on hard disk or on distant server. In the latter case, images can be accessed with remote access protocols such as Samba or NFS.

2.2 Software Equipment

Though most of the methods described in the sequel may be found in several bioimage analysis software, the popular free Fiji platform [1] is recommended unless otherwise needed. Fiji can be installed on the Windows, Mac OS, and Linux platforms. Fiji is written in

Java and will run with preinstalled Java Runtime Environment. If required, a Fiji version with an embedded Java distribution can also be downloaded. Users requiring more than 2 GB RAM usage in Fiji should run on a 64-bit operating system due to limitation in Java memory management on 32-bit systems. The core functionalities of the software can be extended using plugins. Fiji installation bundles a number of preselected plugins, and additional plugins can be added after installation. Fiji and the plugins implementing the methods described below can be found with installation instructions from the imagej.net website.

2.3 File Formats

Acquired images in light microscopy are generally obtained in proprietary formats such as LSM, ZVI, or LIF. Many image analysis software can read these formats. In Fiji, the LOCI BioFormats plugin reads a wide range of file formats used in biological science. Alternative formats not specific to light microscopy can be used as well. File formats supporting lossless compression, such as TIF (from which several proprietary formats such as LSM are derived), are recommended. Formats with lossy compression, such as JPEG, should be avoided for the purpose of scientific image analysis. The adoption of systematic, standardized file naming conventions is strongly recommended.

3 Methods

3.1 Quantifying Biological Information Using Image Analysis

Digital image analysis consists in extracting biologically meaningful information by performing quantitative measurements on acquired images. Of particular interest are the measurements or the so-called *descriptors* with properties that facilitate the reusability and generalization of results. These descriptors are invariant to image transformations (such as translation, rotation, or scaling), robust against noise and image artifacts, and easy to interpret and validate.

The spectrum of quantitative information that can be extracted using image analysis is quite large, ranging from simple measurements such as object numbers to more elaborate ones such as texture descriptors. In this section, we describe the main quantitative measurements and types of analysis that are of special relevance to study biological samples using light microscopy.

Digital images are matrices of pixel (2D) or voxel (3D) values. In acquired images, these values range from 0 to 255 or more, depending on the encoding of intensity signals and image bit-depth. The purpose of image processing is to transform acquired images (Fig. 1a) into images of objects (Fig. 1b), in which values represent labels that typically range from 0 (background) to N (number of objects). Some object measurements can be made using label images only (geometrical parameters); others require to use label images as masks defining where to perform measurements on the original images (photometrical parameters).

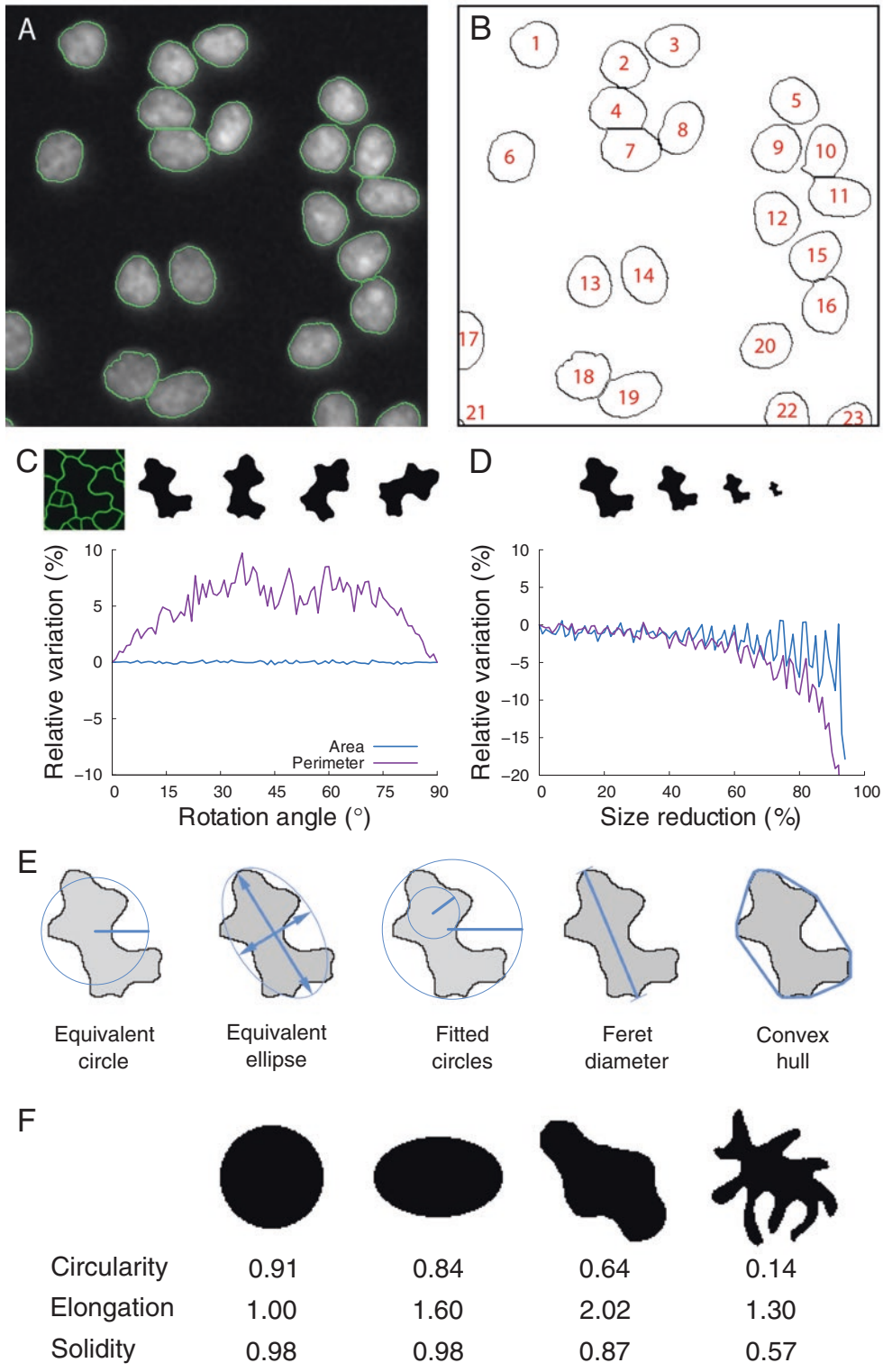

Fig. 1 Morphological and photometric measurements. (**a**) Grayscale light microscopy image (DAPI-stained nuclei). Cell borders are highlighted in *green*. (**b**) Cell boundaries with cell count numbers. (**c**) Influence of rotation on object area and perimeter measurements. (**d**) Influence of scale on object area and perimeter measurements. (**e**) Geometrical features. Many size and shape measurements are derived from the equivalent circle, the equivalent ellipse, the circumscribed and inscribed circles, the Feret diameters, and the convex hull. (**f**) Shape measures for different object shapes

3.1.1 Detecting and Counting Objects

The first information provided by image analysis is the detection and counting of objects of interest (Fig. 1b). This type of information is relatively easy to retrieve, insofar as it does not require a perfect image of object shapes. However, care must be taken when converting object counts to densities if acquired images correspond to sample windows. Corrections for object intersections with image borders must be applied to avoid over- or underestimating densities. Stereology provides methods to compute unbiased estimators from sampled image data [2].

3.1.2 Measuring Sizes and Quantifying Shapes

Other frequently relevant measurements are those related to the size and shape of the objects under study. In image analysis, area is one of the most popular measures of object size. Object area is defined as the product of pixel area by the number of pixels in the object. Pixel area can be computed from the spatial calibration of the images, which gives, in physical distance units, the width and height of a pixel in the real space (*see* **Notes 1** and **2**). Area is a robust size descriptor (Fig. 1c, d). However, at a given spatial calibration, the relative error on area measurement increases when object size decreases (*see* **Note 3**). Image acquisition conditions should be adjusted according to the scale of the smallest objects for which area measurements are desired.

Since it is given in square distance units, area is not easy to interpret. Parameters expressed in distance units may be preferred, such as object perimeter. A straightforward perimeter estimate is obtained from the chain-code representation of object boundary by summing lengths of straight and diagonal moves. This is a biased estimate which in addition is not robust to scale or rotation [3, 4] (Fig. 1c, d). Formulas with statistical corrections terms have been proposed [5]. Unbiased estimates can be obtained using the Crofton formula, which computes the perimeter from the number of intersections between object contour and parallel lines at various orientations [3, 4]. Unfortunately, this perimeter estimation is seldom implemented in bioimaging software [6].

Robust size measurements expressed in distance units can be derived by assimilating objects to ideal shapes (Fig. 1e). The equivalent circular diameter ($\sqrt{4 \times area \div \pi}$) is the diameter of a disk with the same area as the object. Approximating an object with its equivalent inertia ellipsis provides two diameter measures known as major and minor axis lengths. Alternative measures of object extent are provided by the Feret diameters, defined by the spacing at all angles of a virtual caliper rotating around the object. Image analysis software generally report only the largest and the smallest values.

Shape parameters quantify the geometrical information that is independent of absolute size. These measures can be performed even when the spatial calibration of the images is not known (as long as pixels/voxels are square/cubic) because their definitions

encompass a scale normalization. Probably the most popular shape parameter (sometimes called *The Shape Factor*) is circularity ($4 \times \text{area}/\text{perimeter}^2$). Circularity takes its maximum value 1 for a disk and decreases towards 0 when shape complexity increases. Another useful parameter is solidity (area ÷ area of the convex hull), which decreases when shape concavity increases (Fig. 1e; **Note 4**). Solidity is related to the local behavior of the object silhouette. Other parameters capture global shape traits. The most popular is probably elongation, which is computed from the object's equivalent ellipsis (length of largest axis ÷ length of shortest axis). Circularity depends on both global and local shape properties.

Any of these shape parameters only captures some aspects of the object form. Users should be aware of what specific shape features are quantified by different parameters and should remember that shape is never completely represented by these measurements (Fig. 1f). Alternative shape measures, such as Fourier descriptors [7], provide complete representations. However, they are more complex to interpret and are seldom available in bioimaging software.

Size and shape parameters derived by an integration over the entire object, such as equivalent radius and elongation, are generally robust. Conversely, parameters relying on extreme values, such as Feret diameters, are less robust. The popularity of the circularity index is paradoxical, given that this is one of the least robust shape parameters due to its dependence on perimeter (*see* **Note 5**). The drawback of integration-based parameters is that they are not always as easy to interpret and to relate to physical reality.

3.1.3 Quantifying Intensities

Complementary to morphometric parameters, photometric measurements are obtained by quantifying intensity values. They are typically quantiles (minimum, maximum, median) and moments (mean, variance, skewness, kurtosis) of intensity distributions within objects or regions-of-interest. For instance, measuring the total amount of fluorescence on each detected cell in an image can be used to determine cells with high expression of a specific gene. The simplicity of the few measures that are generally made in intensity-based analysis is misleading. It is counterbalanced by the number of issues that can potentially affect measurements [8].

3.1.4 Measuring Positions and Analyzing Spatial Distributions

Object position is frequently represented by the centroid, the point of average coordinates in the image plane (*see* **Note 6**), or by the center-of-mass (intensity-weighted barycenter of object pixels). While absolute positions in the image plane are useful on a control environment, relative positions with respect to other structures are generally more relevant. Euclidean distances or angles can be used for this purpose. Various descriptors such as radial analysis measures are also used to quantify the relative positioning of objects included within other structures [9].

One particular and very popular case of spatial analysis is colocalization analysis. It provides a measure of the spatial co-occurrence between two or more types of objects labeled with different fluorophores. There exist two major ways of performing a colocalization analysis, either by a photometric approach (using coefficients to express the intensity correlation between different channels) or by a geometrical approach (using the overlap between the pre-detected objects). Photometric studies should be conducted with caution since the reliability of the correlation coefficients depends on many factors, including a number of different sources of noise [10, 11].

Based on distance measurements, spatial interactions in the relative positioning of objects can be analyzed using spatial statistics. For example, spatial point pattern analysis [12] provides methods for characterizing the spatial distribution of the objects of interest and to test if they are located at random (independently of each other's location), tend to form clusters (indicating a possible attraction) or follow a regular distribution (which suggests a repulsion among the objects). Furthermore, specific spatial models can be statistically tested to find the distribution that fits best the underlying spatial organization. Spatial statistics are not yet popular in bioimage analysis, probably because they have essentially been developed in the context of ecology and forestry applications. Methods for handling issues specific to biological studies, such as replicated data, arbitrarily sized objects and exhaustive sampling within confined domains, have to be developed [13].

3.1.5 Motion Analysis and Tracking

Motion analysis quantifies the apparent object motion between consecutive images on an image sequence. The simplest application consists on detecting the motion, i.e., the points in the image that are moving. More complex analysis can be performed to group moving points belonging to the same object, determine the motion velocity and direction of each point, or follow specific points or objects over time, which is known as tracking [14].

3.2 Finding Objects in Images: The Segmentation Problem

Prior to analysis, objects must be detected and defined according to a representation suitable for quantification by the computer. This is achieved through segmentation, the process of partitioning an image into multiple homogeneous regions or segments (Fig. 2). Segmentation constitutes a major transition in the image analysis pipeline, replacing intensity values (quantitative information) by region labels (qualitative information). In this section we describe some of the most popular methods for segmenting light microscopy data. The reader should keep in mind that there is no universal segmentation method. It is recommended to try different approaches to determine which one works best for his/her specific image data.

3.2.1 Binarization by Grey Level Thresholding

Binarization, the simplest image segmentation method, consists in classifying pixels into two classes: pixels belonging to objects of

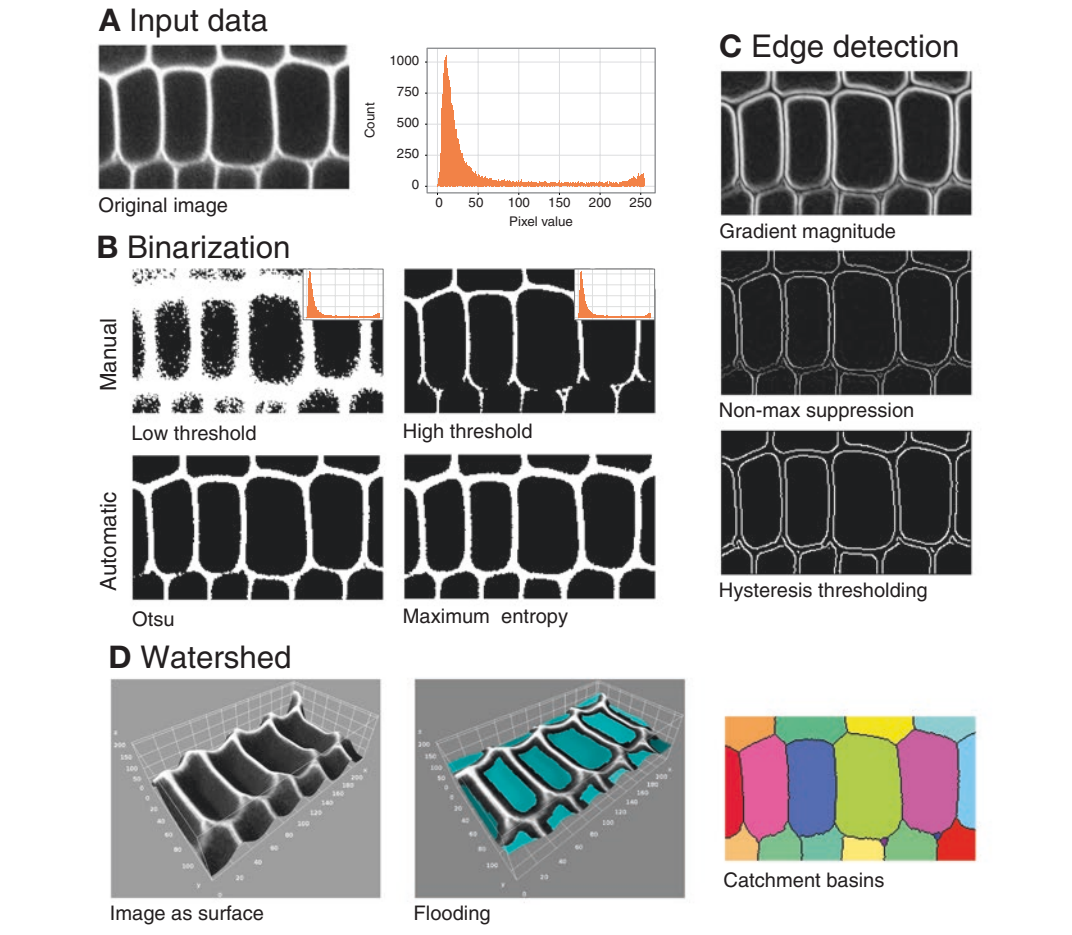

Fig. 2 Segmentation methods. (**a**) Example of input image data and corresponding histogram (crop of confocal *XY* plane of *Arabidopsis* embryo [45]). (**b**) Binarization by thresholding (manual and automatic methods). (**c**) Edge detection by gradient operator, followed by non-maximum suppression and hysteresis thresholding. (**d**) Watershed segmentation by flooding, considering the image as a topographic surface. *Right*: segmentation result. (**e**) Segmentation by active contours/level sets from manually placed seed points. (**f**) Segmentation by pixel classification. A set of pixels is selected for training (*green* and *red markings*), image features are extracted from the original image, the pixels are then represented in the feature space and a classification method is trained and applied to classify all other pixels

interest (*foreground*) and pixels belonging to other parts of the image (*background*). This binary classification is performed by comparing the intensity value of each pixel to a threshold value. All pixels above the threshold are marked as foreground (usually by setting them to white) and the rest of pixels are marked as background (usually black) (Fig. 2b). This approach is very common to segment light microscopy data, especially fluorescence images where the areas of interest are substantially brighter than the rest of the image.

Even under fixed image acquisition conditions, using the same threshold over a collection of images is generally not recommended because of uncontrolled fluctuations in intensity values across images. Hence, a new threshold value should be computed for each image, using an automated threshold selection technique. Some thresholding methods are global and use the same threshold value over the entire image. Local methods adapt the threshold to compensate for regional intensity variations. All automatic thresholding methods consist in optimizing some objective criterion that can be statistical (e.g., maximization of inter-class variance [15] or of entropy [16]), probabilistic (e.g., minimization of pixel classification error [17]) or structural (e.g., circularity of detected objects).

Binarization generates an image where the objects of interest are connected regions of white pixels called connected components. Labeling the different connected components allows distinguishing different objects prior to quantitative analysis (Fig. 1b).

3.2.2 Defining Objects by Their Contours

Sometimes the objects of interest do not have homogeneous intensities but their contours are easily identifiable by their contrast difference with the background. In those cases it might be interesting to use edge detection to segment the images. Edge detection is the process of estimating the boundaries of objects by highlighting places of large intensity variations. This is usually accomplished by calculating the first or second order derivatives of the pixel intensities, followed by thresholding (Fig. 2c). Very frequently additional steps are required to transform those estimations into continuous borders and then close objects.

3.2.3 Watershed Transform

The watershed transform is a popular segmentation method in biological imaging. This method draws an analogy between the image and a topographic surface where bright areas define peaks and dark ones represent valleys. The algorithm simulates the flooding of the surface from water sources placed at its lowest points and builds dams when the water from different sources meet [18]. Each separate region is a *catchment basin* that defines an object, while the separation lines between them are known as *watersheds*.

This approach requires the borders of the regions of interest to be brighter than the background and than the interior of the regions. In light microscopy, it is very frequently applied to data

expressing a membrane marker (Fig. 2d). On images where the whole objects are stained rather than just their boundaries, it is necessary to preprocess the image with an edge detector.

3.2.4 Constraining Segmentation Using Geometrical Knowledge

In some cases, the objects of interest are not completely defined by the information in the image. For example, cell membranes might appear with gaps produced by different problems during the image acquisition. In those cases, it is convenient to apply a segmentation method such as active contours, which makes use of prior knowledge on object shape to geometrically constrain the iterative search of the outline (in 2D) or surface (in 3D) that enclose best the objects [19]. The final contours are a compromise between geometric constraints (continuity, elasticity, flexibility) and the location at strong intensity variations. There exist many variants of this strategy. One of the most popular ones makes use of the level set method to efficiently address the curve propagation and topological changes, advancing the contour like a rubber band until it reaches the object boundaries [20] (Fig. 2e).

3.2.5 Classifying Pixels and Learning Segmentation by Example

Image segmentation can be cast as a pixel classification problem, where each pixel has to be labeled as belonging to one class depending on its similarity (in intensity, position, etc.) with other pixels of the same class. The classification can be unsupervised, i.e., without any guidance, or supervised, where the user provides some samples of each class so the classifier learns how to label the rest of pixels in the image. One of the most popular and fastest unsupervised methods is K-means, that groups pixels into K classes or clusters based on how similar they are to the mean of each cluster. Supervised methods are usually a bit slower, because they need a training phase, but more precise since they mimic the classification by an expert.

All these methods can deal with images having n-dimensional pixel values. Grayscale images have $n = 1$, each pixel bearing a single intensity value, and multichannel images have n equal to the number of channels. For example, it is common to use K-means on RGB images ($n = 3$) to separate objects based on color (*see* **Note 7**). Popular tools have emerged recently to segment microscopy images by combining high-dimensional pixel representations (using predefined image features) and supervised classifiers in an interactive way, where the user introduces new training samples and the segmentation results get updated on-the-fly [21, 22] (Fig. 2f). These methods, while slower than classic clustering methods, provide very robust solutions improved by the continuous user feedback (*see* **Note 8**).

3.3 Post-processing Images to Facilitate Analysis

Prior to analysis, it may be needed to improve the segmented images to correct some errors or to transform the object representation to allow the extraction of desired measurements. Typical corrections at this stage include regularizing object shapes, filling

holes inside the segmented regions (false negatives), removing artifacts in the background (false positives) and rearranging the topology of segmented regions (splitting or merging). It is often necessary as well to extract the contours or the center-lines of the objects to simplify the analysis of their structure. As they operate downstream of segmentation on object rather than on intensity images, these transformations are referred to as post-processing operations. This section describes the most common techniques used at this step.

3.3.1 Shape Operations Using Binary Mathematical Morphology

Mathematical morphology is a theory and a set of methods that operate on objects based on their size and shape [23, 24]. The basic operators are a set of morphological filters that can be combined to provide a large variety of image transforms. They are local filters, in the sense that they consider the neighborhood of each pixel/voxel according to a structuring element of given size and shape.

The base morphological filters are the dilation (background pixels where the structuring element intersects the object are turned to object pixels) and the dual operation of erosion (Fig. 3a). Dilation and erosion are generally used in combination to preserve object sizes. For example, the morphological closing (dilation followed by an erosion) removes background regions smaller than the structuring element. Symmetrically, the morphological opening (erosion followed by a dilation) removes objects smaller than the structuring element (Fig. 3a).

3.3.2 Separation of Touching Objects

Due to the low image resolution of the microscope being used or the limited accuracy of the chosen segmentation method, it is frequent that neighboring objects end up connected and therefore considered as a single object (for instance, two cells or nuclei with a separation smaller than the spatial resolution). Morphological opening can be used to separate objects if the spatial extent of object connections is at least one order of magnitude smaller than object sizes. A popular alternative when object connections are too large consists in applying the distance transform to the binary segmented image and then running the watershed method on its inverse to recover the boundaries between objects. This strategy works very well on convex (circular or elliptical) objects such as cells or nuclei (Fig. 3b).

3.3.3 Filling Holes and Gaps

Mathematical morphology also provides with tools to fill holes within objects or to close gaps between parts of objects that would have been split during segmentation. Morphological closing can be used when the spatial extent of holes and gaps is small. Otherwise, hole filling based on morphological reconstruction (*see* below Subheading 3.4) is generally preferred. In light microscopy images, these operators offer a simple and very fast way to make sure that objects like nuclei do not present holes or that cell membranes are completely closed (Fig. 3c).

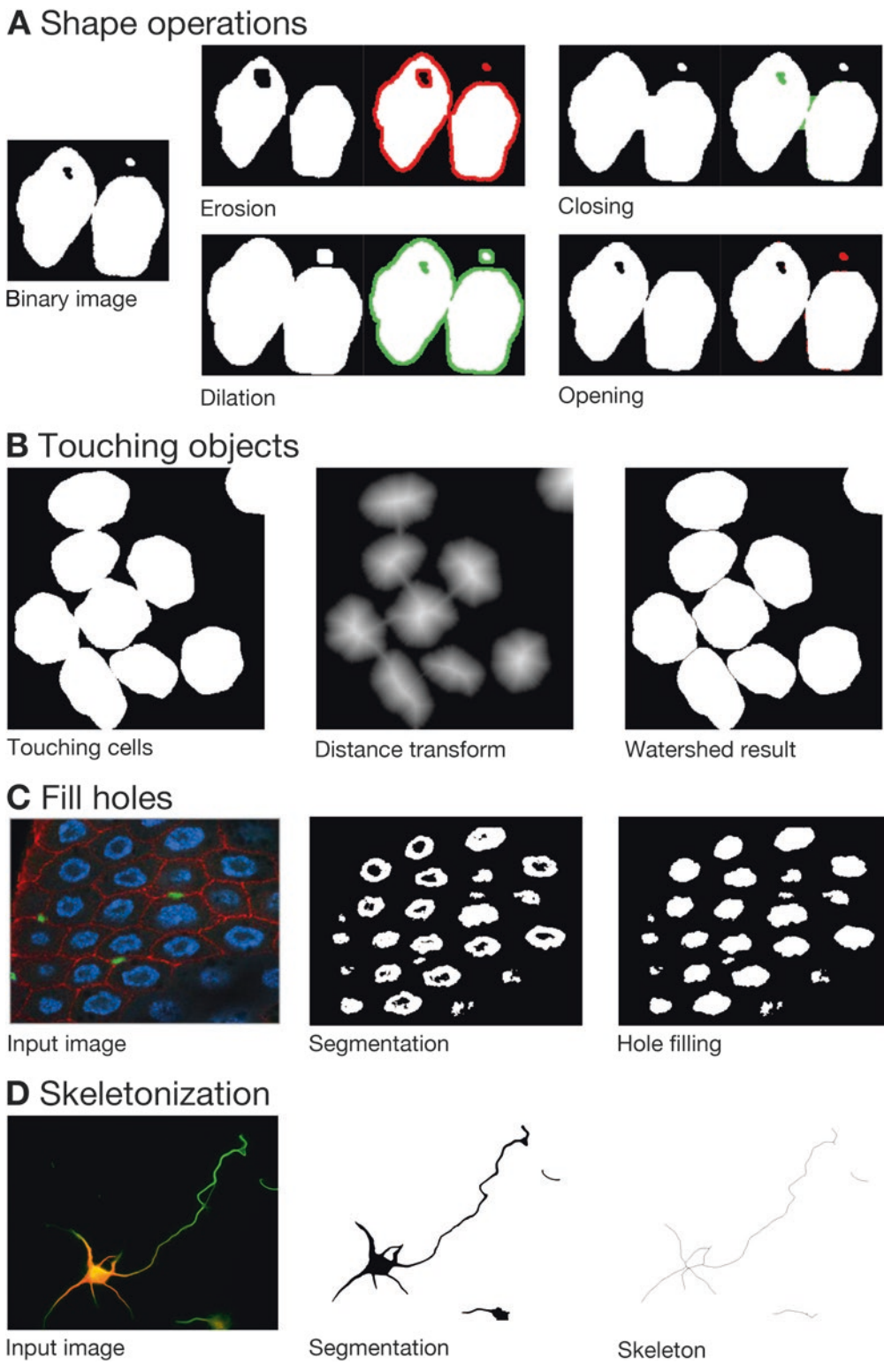

Fig. 3 Post-processing operations. (**a**) Basic morphological operations on a binary image using a 3 × 3 square structuring element. *Red/Green*: object pixels removed/added during operation. (**b**) Separation of touching objects using watershed and distance transform. Watershed was run on the inverted distance map of the binary input image. (**c**) Hole filling applied on a binary segmentation. (**d**) Skeletonization of the binary image of a neuron. Original fluorescence images (**c**, **d**) from the Cell Image Library (CIL39686 and CIL8476 respectively)

3.3.4 Simplifying Shapes Using Skeletonization and Border Thinning

Finally, reducing the representation of objects to pixel-wide skeletons or to contours through morphological operations is a very common strategy to facilitate the analysis of linear structures such as membranes or of treelike organizations such as neuronal arborescences (Fig. 3d).

3.4 Preprocessing Images to Enable Better Object Segmentation

In many applications, it is difficult, if not impossible, to generate a correct image of segmented objects using segmentation and postprocessing operations only. The acquired images must then be filtered to make them easier to process at the segmentation step and onward (*see* **Note 9**). The common principle underlying all preprocessing operators is to increase the separability between object and background pixels. This is achieved either by increasing homogeneity within each class or by increasing the contrast between the two classes.

3.4.1 Increasing Region Homogeneity by Attenuating Noise

Noise is one of the major sources of heterogeneity in input images. Noise can result from the stochastic nature of the sampled physical property (e.g., fluorescence emission) as well as from the acquisition process (thermal, read-out, and quantification noise). Noise induces wide dispersion around histogram peaks and fast fluctuations of intensity values in the spatial domain. At the segmentation step, this potentially hampers the automated detection of correct intensity thresholds and leads to high numbers of background/foreground classification errors.

Standard operators to attenuate noise are spatial linear filters such as the mean and the Gaussian filters (Fig. 4a). These filters replace the value of each pixel by a linear combination of pixel values in its neighborhood. The Gaussian filter is optimal in the case of Gaussian-distributed noise. The degree of smoothing can be tuned by adjusting the size of the neighborhood.

One major drawback of linear filters is that they reduce local contrast by blurring object boundaries. Suboptimal filters that better preserve local contrast may be preferred. The median filter, which replaces each pixel by the median value in its neighborhood, is a popular alternative to linear filters (Fig. 4a). Preserving local contrast can also be achieved by extending neighborhoods from the spatial to the photometric domain. Blurring is then limited by allowing only similar intensities to be combined. Early examples of this approach are the α-trimmed mean and the sigma filters [25]. Adaptive filters such as anisotropic diffusion [26] (Fig. 4a) and bilateral filter [27, 28] were subsequently introduced. Recent developments extended spatial neighborhoods to regions or to the whole image scale, as in the Non-Local Means filter [29], or extended the similarity in the photometric domain from individual values to local patches [30]. The additional cost that comes with most of these adaptive filters compared to classical ones is an increased number of parameters. Identifying the best combination of parameters is therefore more complicated.

3.4.2 Reducing Uncertainty on Object Boundaries by Enhancing Local Contrast

Local contrast corresponds to the slope of an intensity transition at object boundary. A low contrast visually manifests itself by a blurry border. Low contrast is problematic for automatic segmentation because it makes object boundary detection highly sensitive to intensity thresholds. Convolution by the optics of the microscope is the major source of blur in acquired images. Local contrast can be enhanced by subtracting to the image a fraction of its second derivatives, as is classically done using the Laplacian filter or the related unsharp masking operator (Fig. 4b). Deconvolution methods can also be used to remove blur in acquired images [31, 32]. Deconvolution aims at inverting the degradation of the signal that was introduced by the optics of the acquisition system, described by the Point Spread Function (PSF). Theoretical (mathematical model) or empirical (experimentally acquired using fluorescent beads) PSF are used as input in deconvolution methods.

3.4.3 Trade-off Between Preprocessing Operations

Smoothing filters reduce noise but may also reduce local contrast. Conversely, filters enhancing local contrast may increase intensity fluctuations caused by noise. A practical consequence is that a trade-off has to be made between noise reduction and local contrast enhancement and that defects cannot be completely removed from acquired images. It is therefore highly recommended to optimize the conditions of image acquisition to limit as much as possible the need for preprocessing operations (*see* **Note 10**).

3.4.4 Specifically Enhancing Objects of Interest

Noise and contrast filters are applied to reduce defects in images. Preprocessing operations can also be applied to specifically enhance the objects of interest at the expense of other structures. Mathematical morphology on gray level images provides a large spectrum of tools for this purpose [24].

As in the binary case (Subheading 3.3.1), gray level mathematical morphology relies on two basic operations, erosion and dilation, that are applied in tandem in the composite opening and closing operations. In their simplest form, grayscale erosion and dilation consist in replacing each pixel by the minimum (resp. maximum) value over its neighborhood (*see* **Note 11**). Neighborhood size and shape (structuring element) are arbitrary but usually correspond to a discretized version of a disk. Generalizing their binary counterparts, grayscale opening and closing respectively remove bright and dark objects smaller than the structuring element (Fig. 4c).

Small objects such as vesicles are frequently of interest in microscope image analysis. The top-hat transform generates an image where only small bright objects are retained, by subtracting to the original image the result of its opening (dark objects are similarly specifically enhanced by subtracting the original image to the result of its closing) (Fig. 4c). Top-hat is a particular case of background removal techniques, which allow to correct for intensity variations due to uneven illumination over the image (Fig. 4d).

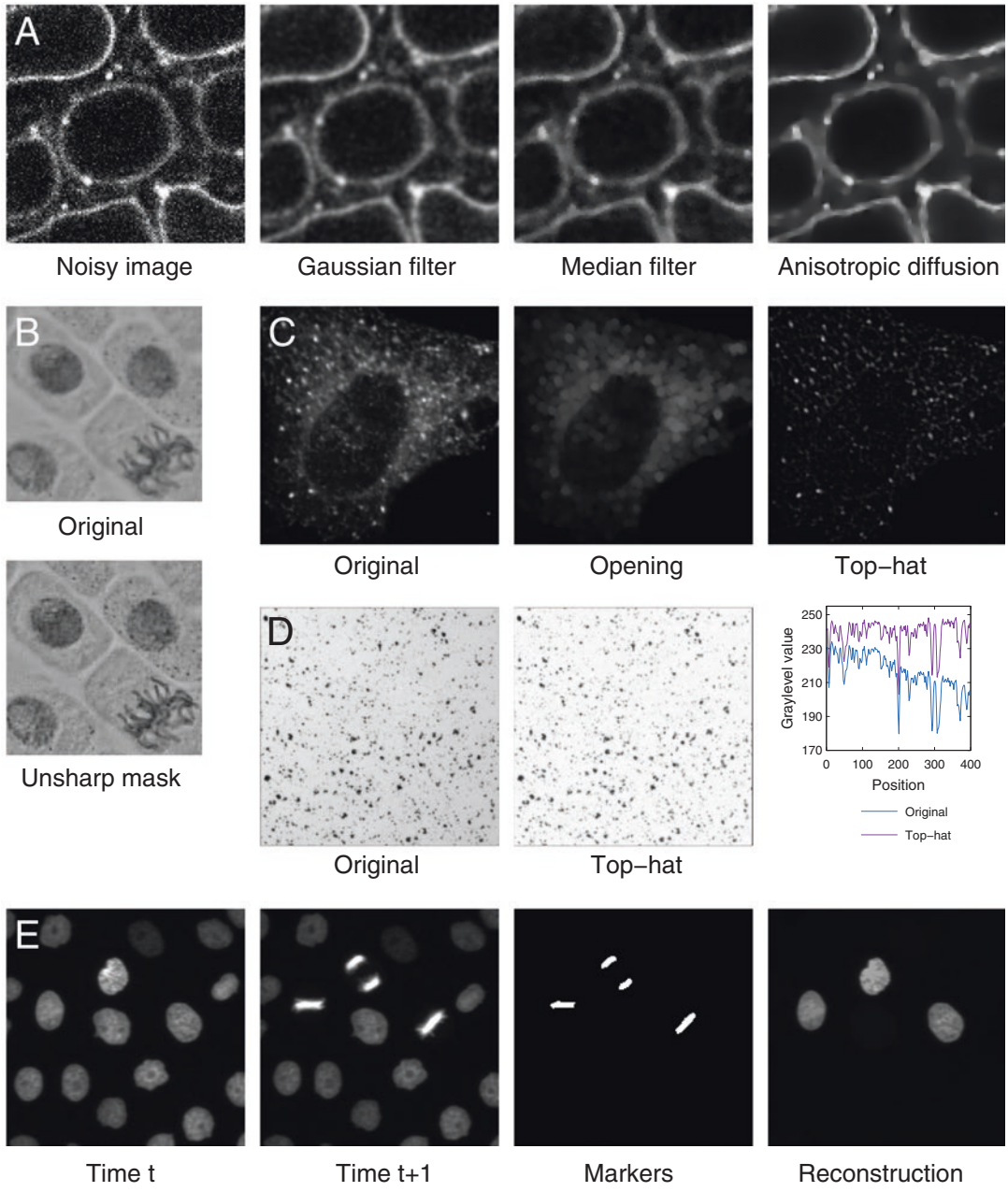

Fig. 4 Preprocessing operations. (**a**) Noise attenuation by spatial filters. Image by S. Vernhettes, INRA Versailles, France. (**b**) Blur removal (local contrast enhancement) using the unsharp mask filter. Original image from the Cell Image Library (CIL43552). (**c**) Size-based object enhancement using the top-hat transform. Small vesicles were enhanced (*right*) by subtracting from the original image (*left*) its morphological opening (*middle*). Original image from the Cell Image Library (CIL13568). (**d**) Background correction using the top-hat transform. The uneven illumination was removed by subtracting the original image from its morphological closing. The graph shows graylevel profiles along the horizontal midline in both images. (**e**) Marker-based object enhancement and selection using gray level morphological reconstruction. Reconstruction was used to find in an image sequence the nuclei at time t that have divided at time $t+1$. The markers were obtained by thresholding image at $t+1$ and were used for the reconstruction by dilation of image at t. Original image from http://www.codesolorzano.com/celltrackingchallenge/Cell_Tracking_Challenge/Datasets.html [46]

Geodesic reconstruction is another class of powerful mathematical morphology operators that can be used to filter objects in an image (called the mask) based on markers in another image [33]. Markers in this context refer to sets of pixels that tag the objects of interest. Reconstruction by dilation proceeds by repeatedly dilating the marker image while constraining it to remain below the mask image. When stability is reached, the marker image contains a reconstructed version of the objects in which markers where initially located (Fig. 4e). Many other useful operations are defined based on geodesic reconstruction, including the removal of peaks of height below a threshold (h-maxima transform) or the imposition of minima at specified positions. The latter operation is used as a preprocessing step in the marker-based watershed. It greatly contributes to improve the watershed segmentation results by limiting the amount of over-segmentation. Due to the frequent use of multiple channels corresponding to as many experimental labels, geodesic operations are particularly suited for processing biological images acquired using light microscopy. Unfortunately, they are not frequently available in bioimage analysis software [6]. The same holds for other classes of mathematical morphology operators such as area and other attribute openings [34].

3.5 Validation of Image Analysis Pipeline and Results

Several factors can affect the validity of measurements obtained with an automated image processing and analysis pipeline. The presence of noise can lead to false-positive detection of objects; an incorrect intensity threshold affects size measurements; programming errors (e.g., in user-defined macros) can lead to incorrect values; etc. Results of quantitative analysis should systematically be examined critically and checked through a validation procedure. The validation process can also be applied at intermediate stages in the pipeline, such as the segmentation step.

The most common validation strategy is to compare the results obtained with the image analysis pipeline to a set of reference measurements (*gold-standard*) obtained by manual analysis of sample images by a human expert. How the comparison between automatic and expert results is performed largely depends on the type of measurement and the image processing step at which evaluation is done. Object counts are typically evaluated using a correlation criterion. Evaluation at the segmentation stage is generally performed by quantifying the overlap between automatic and manual segmentation masks, using criteria such as the Jaccard or Dice coefficients [35, 36]. The limit of this evaluation strategy is that human expertise is itself affected by uncertainty due to intra- and inter-operator variability. Another limitation is that it is not always possible in practice to manually generate a dataset of sufficient size, as for example to validate a 3D segmentation.

An alternative validation strategy consists in using image simulation algorithms to generate a gold standard. Given models of

object geometries and of the physics of the image formation process (microscope characteristics such as PSF, geometrical and photometrical alterations such as noise, etc.), algorithms can be used to generate artificial images that simulate real images of cells or particles [37, 38]. Model parameters can be set arbitrarily and adjusted by trials-and-errors. Alternatively, they can also be learned from sample images [39]. The usefulness of such image generators of course depends on the ability to model accurately the biological structures and the physical processes that determine image contents.

Lastly, image measurements can be compared and cross-validated with results obtained using alternative experimental methods than image analysis. However, a few numbers of measurements can be validated along this approach (such as concentration of molecules in ratiometric fluorescence imaging), given that many parameters can hardly be obtained using other methods than image analysis (e.g., shape measurements).

When validation based on a gold standard is not feasible, confidence on the obtained results can be quantitatively assessed by evaluating the sensitivity of measurements to the parameter setup in the image analysis pipeline. Due to the possibly large number of parameters and to the resulting combinatorial explosion, this approach is however applicable to a limited number of parameters, such as threshold values at the segmentation step [40].

3.6 The Whole Picture: A Goal-Oriented, Iterative Approach

The previous sections presented the building blocks (ingredients) of a typical image processing and analysis pipeline. This section presents a goal-oriented generic strategy (recipe) to assemble these elements and instantiate them in practice. Designing an image analysis solution is not a one-pass process. It generally proceeds by trial-and-error and involves several rounds before converging to a final solution. Since it is generic, the "algorithm" for pipeline design presented here is of course to some extent idealized. It is intended as a general guideline for rationalizing and optimizing the design of image analysis pipelines. A key point of the proposed methodology is that it does not follow the chronological order of operations in the final pipeline, but instead proceeds backwards from the analysis objective (Fig. 5).

1. Step 1 is to specify formally the analysis objectives by identifying the quantitative measurements to perform. At this stage, the objectives are translated from the biological to the mathematical or computer science terminology. For example, "nucleus position" or "cell shape" are ambiguous terms for image analysis; "centroid" or "solidity," for example, should be used instead. Care should be taken that the chosen parameters actually and faithfully quantify the biological features of interest (*see* comments and notes in Subheading 3.1).

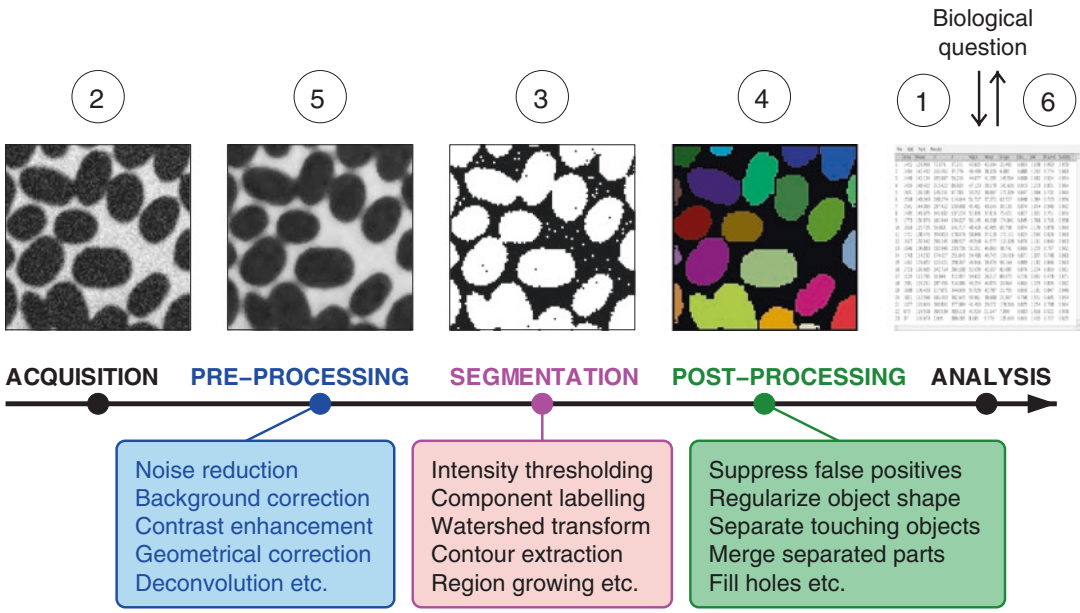

Fig. 5 Main steps in a generic image processing and analysis pipeline. Typical operations performed at each processing step are mentioned in the related *box*. *Circled numbers* refer to the ordering in which the different steps are progressively introduced in the proposed strategy (*see* Subheading 3.6)

2. Step 2 is to perform image acquisition using appropriate conditions given the objectives defined at **step 1**. A first important point to consider at this stage is a sufficient resolution for the desired measurements (*see* Subheading 3.1). Optical resolution primarily depends on the numerical aperture of the objective and on light wavelength. The pixel size should be not set arbitrarily but small enough to preserve the resolution of the microscope image. It can generally be set by microscope software to its optimal value given the imaging conditions, following the Nyquist–Shannon criterion [41] (*see* **Note 12**).

   A second important point is to ensure the largest possible range of intensity values in the acquired images while preventing saturation at both ends of the dynamic range (*see* Subheading 3.2). On a confocal microscope, this is obtained by tuning the gain of the photomultiplier (*see* Note 13). When acquiring collections of images, a trade-off has to be found to meet this requirement while at the same time keeping acquisition conditions constant.

   A final important point is to improve as much as possible the signal-to-noise ratio to ease the segmentation step (*see* Subheading 3.2) and to limit the needs for preprocessing operations (*see* Subheading 3.4). On a confocal microscope, this can be tuned by adjusting the laser power, the pinhole aperture and the total time spent on each pixel [42]. Trade-offs have to be made, since for example longer exposure times and increased laser power may induce other issues such as photobleaching and photodamage.

3. Step 3 is to perform image segmentation using one of the methods presented in Subheading 3.2. Which method to use depends on the origin of the contrast that defines the objects of interest. However, image thresholding is frequently an appropriate initial choice in light microscopy because of the use of extrinsic labeling. If a correct segmentation is obtained, then go to **step 6**. Otherwise, go to **step 4**.
4. Step 4 is to remove moderate errors in the images of segmented objects, using the post-processing techniques presented in Subheading 3.3. If post-processing is sufficient to generate a correct image of objects, then go to **step 6**. Otherwise, go to **step 5**.
5. Step 5 is to enhance acquired images using the preprocessing techniques presented in Subheading 3.4 to make them easier to process at the subsequent segmentation and post-processing steps. Given that the less image transformations, the better, preprocessing should be considered only when everything else (segmentation and post-processing) fails at producing correct object images.

   There is generally a mix of degradation in acquired images. Diagnosing the most important ones and among them, those that make segmentation difficult, is essential to select the appropriate operators that should be applied at this stage. Simple tools such as variance of local histograms within structurally homogeneous regions and gray level profiles can be used to evaluate noise levels and local contrast.

   Validating preprocessing operations is more difficult than segmentation and post-processing steps, because they involve intensity rather than label images. The validity of a preprocessing operation is therefore evaluated based on the success it confers to the downstream segmentation and post-processing steps.

   Generally, several rounds of **steps 3–5** sequences will be applied before converging to a satisfactory pipeline. In some situations, it will not be possible to generate correct object images from the input images. In such a case, go to **step 2** to reconsider sample preparation and image acquisition conditions.
6. Step 6, the final step, is to run the image analysis proper by performing on the segmented objects the measurements defined at **step 1**. There is no practical recommendation at this stage except the ones already formulated in Subheading 3.1.

4 Notes

1. In biological imaging, the spatial calibration of an image is typically expressed in μm or nm. It is frequently interpreted as the size of the square covered by a pixel in the real space.

Actually, spatial calibration refers to the spacing between consecutive pixels. Pixel width and height are generally identical on modern image acquisition instruments.

2. Pixel calibration is generally stored automatically by acquisition systems in the meta-data section of the image files and can be read by most image analysis software. It is however good practice to check that this is indeed the case. In ImageJ/Fiji, this information appears in *Image→Properties…*.
3. In practice, image analysis software will report areas for any object size. It is not recommended to rely on area values for objects smaller than 5–10 pixels in diameter, given the large relative uncertainty that may affect these measures.
4. There is ample room for confusion in the nomenclature of shape parameters. The same definition is frequently referred to under different names (for example, circularity is also known as compactness; elongation may be called aspect ratio). The same name can also refer to different parameter definitions (e.g., the inverse formula is sometimes used for circularity). Lastly, the vocabulary, that mostly originates from material science, may be inappropriate in biology. For example, solidity actually quantifies shape convexity, and would probably be better referred to as such in a biological context. In any case, we advise to systematically check the actual definitions of size and shape parameters reported by image analysis software.
5. We recommend using the solidity parameter rather than circularity everywhere possible. Though it depends on the extreme points of object silhouette, solidity is more robust since it relies on area measurements only (object and convex hull). A robust alternative to the classical circularity measure was proposed in [43].
6. The centroid of an object is not systematically a representative point of this object. The centroid can be located outside an object with a non-convex shape. Alternatives such as the ultimate eroded point may be preferred in such situations.
7. The Ridler and Calvard thresholding technique available as the default method in the ImageJ/Fiji software is a special case of K-means clustering, run with $K=2$ in the 1-dimensional space of grayscale values. It is also an iterative version of Otsu's method [44].
8. The speed of the interactive learning segmentation depends on the number and size of the selected image features and the choice of the classifier method. In the Trainable Weka Segmentation plugin [22] of Fiji [1], these parameters can be tuned in the settings dialog. We recommend to start with the default configuration and to set the maximum sigma to a radius larger than the structures that can be confused with objects at a pixel level (for example the radius of bright spots when the

aim is to segment membranes). The number of features can be reduced to save computer memory and calculation time when the segmentation accuracy does not get affected.

9. We only consider in this section preprocessing operations that enhance the image in the perspective of segmentation. Techniques improving the visual appearance of images for display purposes, such as histogram transforms, are generally not to be applied in an automated image processing and analysis pipeline and are therefore not considered in this chapter.
10. Ideally, all preprocessing would be taken care of at the image acquisition stage. Investing time to optimize sample preparation, mounting, and microscope setup is highly beneficial for the subsequent image processing steps.
11. The general definition of erosion and dilation operations actually involves minimum and maximum after point-wise subtraction or addition to neighboring pixels of intensity values stored in a structuring element. This reduces to mere minimum and maximum operations when these values are constant ("flat" structuring element). Using a non-flat structuring element brings robustness to noise. The use of such elements has become less popular since the introduction of the powerful reconstruction operators, which rely on minimum and maximum operations only.
12. It is generally recommended to set pixel/voxel size 2–3 times smaller than optical resolution. For identical acquisition conditions, optimal values reported by different microscope software can vary due to the different formulas used to compute resolution from numerical aperture and wavelength.
13. The offset parameter is sometimes used to remove background noise, setting the corresponding pixel values to zero. When images are acquired to be digitally processed and analyzed, this is not necessary. This may even be detrimental since background noise may be useful for some preprocessing or segmentation operators (for example, for estimating a noise level).

References

1. Schindelin J, Arganda-Carreras I, Frise E et al (2012) Fiji: an open-source platform for biological-image analysis. Nat Methods 9:676–682
2. Howard CV, Reed MG (1988) Unbiased stereology: three-dimensional measurement in microscopy. BIOS Scientific Publishers, Oxford
3. Pirard E, Dislaire G (2005) Robustness of planar shape descriptors of particles. Proc. Int. Assoc. Math. Geol. Conf. Toronto, CA
4. Lehmann G, Legland D (2012) Efficient N-dimensional surface estimation using Crofton formula and run-length encoding. Insight J. http://hdl.handle.net/10380/3342
5. Dorst L, Smeulders AWM (1987) Length estimators for digitized contours. Comput Vis Graph Image Process 40:311–333. doi: http://dx.doi.org/10.1016/S0734-189X(87)80145-7
6. Legland D, Arganda-Carreras I, Andrey P (2016) MorphoLibJ: mathematical morphol-

ogy library for ImageJ. Release 1(2):2. doi:10.5281/zenodo.51734
7. Pincus Z, Theriot JA (2007) Comparison of quantitative methods for cell-shape analysis. J Microsc 227:140–156. doi:10.1111/j.1365-2818.2007.01799.x
8. Waters JC (2009) Accuracy and precision in quantitative fluorescence microscopy. J Cell Biol 185:1135–1148. doi:10.1083/jcb.200903097
9. Ronneberger O, Baddeley D, Scheipl F et al (2008) Spatial quantitative analysis of fluorescently labeled nuclear structures: problems, methods, pitfalls. Chromosom Res 16:523–562
10. Bolte S, Cordelieres FP (2006) A guided tour into subcellular colocalization analysis in light microscopy. J Microsc 224:213–232
11. Dunn KW, Kamocka MM, McDonald JH (2011) A practical guide to evaluating colocalization in biological microscopy. Am J Physiol Physiol 300:C723–C742
12. Diggle PJ (2014) Statistical analysis of spatial and spatio-temporal point patterns, 3rd edn. Chapman and Hall/CRC Press, Boca Raton
13. Andrey P, Kiêu K, Kress C et al (2010) Statistical analysis of 3D images detects regular spatial distributions of centromeres and chromocenters in animal and plant nuclei. PLoS Comput Biol 6:e1000853
14. Meijering E, Smal I, Danuser G (2006) Tracking in molecular bioimaging. IEEE Signal Process Mag 23:46–53. doi:10.1109/MSP.2006.1628877
15. Otsu N (1979) A threshold selection method from gray-level histograms. IEEE Trans Syst Man Cybern 9:62–66
16. Kapur JN, Sahoo PK, Wong AKC (1985) A new method for gray-level picture thresholding using the entropy of the histogram. Comput Vis Graph Image Process 29:273–285
17. Kittler J, Illingworth J (1986) Minimum error thresholding. Pattern Recognit 19:41–47
18. Vincent L, Soille P (1991) Watersheds in digital spaces: an efficient algorithm based on immersion simulation. IEEE Trans Pattern Anal Mach Intell 13:583–598
19. Kass M, Witkin A, Terzopoulos D (1988) Snakes: active contour models. Int J Comput Vis 1:321–331
20. Sethian JA (1999) Level set methods and fast marching methods: evolving interfaces in computational geometry, fluid mechanics, computer vision, and materials science. Cambridge University Press, Cambridge
21. Sommer C, Straehle C, Koethe U, Hamprecht FA (2011) ilastik: interactive learning and segmentation toolkit. In: 2011 IEEE international symposium on biomedical imaging: from nano to macro, pp 230–233
22. Arganda-Carreras I, Cardona A, Kaynig V, Schindelin J (2011) Trainable weka segmentation. Fiji website
23. Serra J (1982) Image analysis and mathematical morphology. Academic Press, London
24. Soille P (2003) Morphological image analysis: principles and applications, 2nd edn. Springer-Verlag, Berlin, Germany
25. Lee J-S (1983) Digital image smoothing and the sigma filter. Comput Vis Graph Image Process 24:255–269. doi: http://dx.doi.org/10.1016/0734-189X(83)90047-6
26. Perona P, Malik J (1990) Scale-space filtering and edge detection using anisotropic diffusion. IEEE Trans Pattern Anal Mach Intell 12:629–639
27. Tomasi C, Manduchi R (1998) Bilateral filtering for gray and color images. In: Sixth Int. Conf. Comput. Vis. pp 839–846
28. Smith SM, Brady JM (1997) SUSAN—a new approach to low level image processing. Int J Comput Vis 23:45–78
29. Buades A, Coll B, Morel J-M (2005) A review of image denoising algorithms, with a new one. Multiscale Model Simul 4:490–530
30. Kervrann C, Boulanger J (2006) Optimal spatial adaptation for patch-based image denoising. IEEE Trans Image Process 15:2866–2878
31. Wallace W, Schaefer LH, Swedlow JR (2001) A workingperson's guide to deconvolution in light microscopy. Biotechniques 31:1076–1097
32. Cannell MB, McMorland A, Soeller C (2006) Image enhancement by deconvolution. In: Pawley BJ (ed) Handb. Biol. Confocal Microsc. Springer, Boston, MA, pp 488–500
33. Vincent L (1993) Morphological grayscale reconstruction in image analysis: applications and efficient algorithms. IEEE Trans Image Process 2:176–201
34. Breen EJ, Jones R (1996) Attribute openings, thinnings, and granulometries. Comput Vis Image Underst 64:377–389. doi: http://dx.doi.org/10.1006/cviu.1996.0066
35. Jaccard P (1912) The distribution of the flora in the alpine zone. New Phytol 11:37–50
36. Dice LR (1945) Measures of the amount of ecologic association between species. Ecology 26:297–302
37. Lehmussola A, Ruusuvuori P, Selinummi J et al (2007) Computational framework for simulating

fluorescence microscope images with cell populations. IEEE Trans Med Imaging 26:1010–1016. doi:10.1109/TMI.2007.896925

38. Svoboda D, Kozubek M, Stejskal S (2009) Generation of digital phantoms of cell nuclei and simulation of image formation in 3D image cytometry. Cytom A 75:494–509. doi:10.1002/cyto.a.20714
39. Murphy RF (2016) Building cell models and simulations from microscope images. Methods 96:33–39. doi:10.1016/j.ymeth.2015.10.011
40. Eils R, Dietzel S, Bertin E et al (1996) Three-dimensional reconstruction of painted human interphase chromosomes: active and inactive X chromosome territories have similar volumes but differ in shape and surface structure. J Cell Biol 135:1427–1440
41. Pawley JB (2006) Points, pixels, and gray levels: digitizing image data. In: Pawley BJ (ed) Handb. Biol. Confocal Microsc. Springer, Boston, MA, pp 59–79
42. Sheppard CJR, Gan X, Gu M, Roy M (2006) Signal-to-noise ratio in confocal microscopes. In: Pawley BJ (ed) Handb. Biol. Confocal Microsc. Springer, Boston, MA, pp 442–452
43. Žunić J, Hirota K, Rosin PL (2010) A Hu moment invariant as a shape circularity measure. Pattern Recognit 43:47–57. doi: http://dx.doi.org/10.1016/j.patcog.2009.06.017
44. Xue J-H, Zhang Y-J (2012) Ridler and Calvard's, Kittler and Illingworth's and Otsu's methods for image thresholding. Pattern Recognit Lett 33:793–797. doi:10.1016/j.patrec.2012.01.002
45. Bassel GW, Stamm P, Mosca G et al (2014) Mechanical constraints imposed by 3D cellular geometry and arrangement modulate growth patterns in the Arabidopsis embryo. Proc Natl Acad Sci U S A 111:8685–8690
46. Maška M, Ulman V, Svoboda D et al (2014) A benchmark for comparison of cell tracking algorithms. Bioinformatics 30:1609–1617. doi:10.1093/bioinformatics/btu080